Journal of Alloys and Compounds, 185 (1992) 353–362
JALCOM 234

Local volume potentials for actinide metals

S. P. Chen
Theoretical Division, Los Alamos National Laboratory, Los Alamos, NM 87544 (USA)

(Received October 8, 1991; in final form January 20, 1992)

Abstract

We have generated *preliminary* local volume potentials with a self-looping fitting procedure for the actinide metals thorium and plutonium based on the available experimental data of their cohesions and lattice constants and estimates of elastic constants and vacancy energies. This effort is an attempt to model the mechanical and transport properties and the stability of phases of these actinide metals under various pressures and temperatures. The successes and deficiencies will be discussed.

1. Introduction

In order to study theoretically the properties of actinide metals such as thorium and plutonium under various pressures and temperatures [1–7], we need to model these metals using molecular dynamics or Monte Carlo methods. These methods require efficient and simplified descriptions of the interactions between atoms, but no simple potentials of these metals exist.

We try to describe the interaction between Th atoms or Pu atoms by using a local volume potential (LVP) [8] which is closely related to the embedded atom method (EAM) of Daw and Baskes [9]. The details of the form and fit of the potential have been described elsewhere [8, 10, 11]; we only present a summary here.

The energy of a homonuclear system of n atoms is written as

$$E = \sum_{i}^{n} E_i \tag{1}$$

where the energy of atom i is given by

$$E_i = \tfrac{1}{2}\sum \phi(r_{ij}) + F[\rho_i] \tag{2}$$

Here r_{ij} is the distance between atoms i and j, ϕ is a pairwise interaction potential and ρ_i is the "electron density" at atom i due to all its neighbors,

$$\rho_i = \sum \rho(r_{ij}) \tag{3}$$

The embedding energy $F[\rho_i]$, which depends only on the local volume (or density), can be interpreted as the energy arising from embedding atom i in an electron gas of density ρ_i. To first order, this embedding energy

0925-8388/92/$5.00

contains all, and only, the quantum mechanical interaction between the embedded atom and the host [12], leaving the pairwise potential to account for the classical electrostatic interaction. To roughly mimic the shape of the classical electrostatic interaction between two frozen, neutral atoms while allowing fitting flexibility, $\phi(r)$ is taken to be a Morse potential,

$$\phi(r) = D_M\{1 - \exp[-\alpha_M(r - R_M)]\}^2 - D_M \tag{4}$$

The three parameters D_M, R_M and α_M define the depth, the distance to the minimum and a measure of the curvature near the minimum respectively. The density function $\rho(r)$ is taken as

$$\rho(r) = r^6[\exp(-\beta r) + 512\ \exp(-2\beta r)] \tag{5}$$

where β is an adjustable parameter. This is the density (ignoring normalization) of a hydrogenic 4s orbital, with the second term added to ensure that $\rho(r)$ decreases monotonically with r over the whole range of possible interaction distances. The 4s shape is chosen to be appropriate for a first-row transition metal and is found to work well for many f.c.c. [13, 14], b.c.c. [15] and h.c.p. [16] metals.

Following Foiles and coworkers [17, 18], $F[\rho]$ is specified by requiring that the energy of the f.c.c. crystal behaves properly as the lattice constant is varied. Rose *et al.* [19] have shown that the cohesive energy of most metals can be scaled to a simple universal function, which is approximately

$$E_U(a^*) = -E_0(1 + a^*)\ \exp(-a^*) \tag{6}$$

where a^* is a reduced distance variable and E_0 is the depth of the function at the minimum ($a^* = 0$). The appropriate scaling is obtained by taking E_0 as the equilibrium cohesive energy of the solid (E_{coh}) and defining a^* by

$$a^* = \frac{a/a_0 - 1}{(E_{coh}/9B\Omega)^{1/2}} \tag{7}$$

where a is the lattice constant, a_0 is the equilibrium lattice constant, B is the bulk modulus and Ω is the equilibrium atomic volume. Thus, knowing E_{coh}, a_0 and B, the embedding function is defined by requiring that the crystal energy from eqn. (6) match the energy from eqn. (2) for all values of a^*. By fitting $F[\rho]$ in this way, the potential should behave properly over a large range of densities.

To be suitable for use in molecular dynamics and molecular statics simulations, the interatomic potential and its first derivatives with respect to nuclear coordinates should be continuous for all geometries of the system. This is accomplished by forcing $\phi(r)$, $\phi'(r)$, $\rho(r)$ and $\rho'(r)$ to go smoothly to zero at $r = r_{cut}$ (as discussed in ref. 8), with r_{cut} optimized in the fitting procedure. So that $F[\rho]$ is properly defined in eqn. (9), $E_U(a^*)$ is also modified to go smoothly to zero when the expanded crystal has a nearest-neighbor distance equal to r_{cut}.

Given the above functional forms for $\phi(r)$ and $\rho(r)$, the five parameters R_M, D_M, α_M, β and r_{cut} are determined by minimizing the deviation between

the calculated and experimental values for the three cubic elastic constants (C_{11}, C_{12} and C_{44}), the vacancy formation energy (E_{vac}) and the bond length (R_0) and bond energy (D_0) of the diatomic molecule and by requiring that the h.c.p. and b.c.c. crystal structures be less stable than f.c.c. Note that because of the way $F[\rho]$ is determined and because it is re-computed for each new choice of the five parameters defining $\phi(r)$ and $\rho(r)$, the potential always gives a perfect fit to the experimental values of E_{coh}, a_0 and B.

2. Potentials for α-Th

We have used the procedure described above to generate LVPs for thorium based on the experimental data of the lattice constants of α-Th and β-Th [20], the cohesive energy of α-Th [21] and the elastic constants [22] (Tables 1 and 2). The results of the fit and some calculated properties are listed in Table 2 and Fig. 1. The r.m.s. deviation of the fit is 0.3%. The LVP fits the f.c.c. and b.c.c. thorium reasonably well. In addition to the results on the f.c.c. phase, we also calculate the vacancy energy of α-Th to be 3.085 eV. The elastic constants of β-Th (b.c.c. phase) and the vacancy energy (2.988 eV) are also listed in Table 2. β-Th has a smaller cohesive energy than α-Th by 0.47 eV, but they have about the same bulk modulus (0.5874×10^{12} dyn cm^{-2} for β-Th *vs.* 0.5801×10^{12} dyn cm^{-2} for α-Th). These results can be checked by total energy band structure calculations or by experimental measurements. We have also calculated the surface energies of several low index planes (see Table 5), namely the (111), (100), (110) and (210) surfaces of α-Th. We found that the (111) surface has the lowest energy (1860 mJ m^{-2}) while (210) has the highest energy (2013 mJ m^{-2}). The surface energies of α-Th are about 20% higher than the estimate of 1550 mJ m^{-2} for α-Th using Miedema's scheme [23] (see Table 5). The agreements between calculated results and the estimate of surface energies are reasonable. The surfaces with 1×2 missing row reconstructions on the (110) and (210) surfaces of α-Th are not favored in our calculations, as shown in Table 5. The predictions of no 1×2 reconstruction on the (110) and (210) free surfaces are not yet verified experimentally (see refs. 13 and 14 and references cited therein).

TABLE 1

Structural properties of thorium [20]. The melting temperature of thorium is 1755 °C and the boiling temperature is 4788 °C [20]

Element	Temperature (°C)	Pressure	Pearson symbol	Space group	Strukurbericht designation	Prototype	Lattice parameter (Å) a
α-Th	25	Atm.	*cF*4	*Fm*3*m*	A1 (f.c.c.)	Cu	5.0842
β-Th	> 1360	Atm.	*cI*2	*Im*3*m*	A2 (b.c.c.)	W	4.11

TABLE 2
Experimental and estimated data of thorium and fitted results of local volume potentials. The r.m.s. deviation of the fit is 0.3%

Property	Exp.	Fit or calc.	Deviation
α-Th phase (f.c.c.)			
a_0 (Å)	5.080	5.080	Exact
E_c (eV)	5.926	5.926	Exact
B (10^{12} dyn cm^{-2})	0.5801	0.5801	Exact
C_{11}	0.7770	0.7782	+0.16%
C_{12}	0.4820	0.4811	−0.19%
C_{44}	0.5110	0.5107	−0.05%
E_{vac} (eV)	–	3.085	–
β-Th phase (b.c.c)			
a_0 (Å)	4.110	4.083	−0.66%
E_c (eV)	–	5.879	–
B (10^{12} dyn cm^{-2})	–	0.5784	–
C_{11}	–	0.6547	–
C_{12}	–	0.5403	–
C_{44}	–	0.6293	–
E_{vac} (eV)	–	2.988	–
D_0 (eV) of diatomic	–	1.169	–
R_0 (Å) of diatomic	–	3.255	–

Local volume potential parameters for Th are: $D_M = 4.8463731$ eV, $R_M = 2.23653$ Å, $\alpha_M = 0.808975$ Å^{-1}, $\beta = 2.02639$ Å^{-1}, $r_{cut} = 8.80861$ Å.

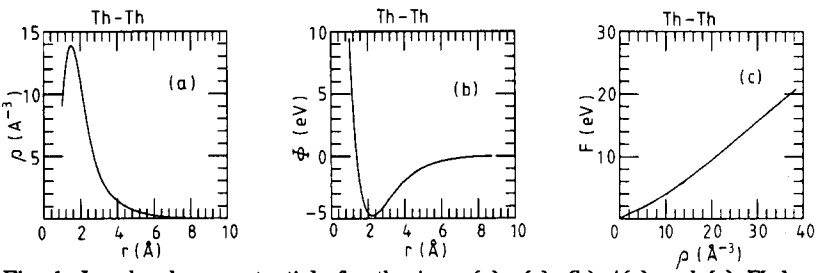

Fig. 1. Local volume potentials for thorium: (a) $\rho(r)$, (b) $\phi(r)$ and (c) $F[\rho]$.

3. Self-looping fitting procedures and the potential for δ-Pu

We have chosen to fit the LVP to the f.c.c. and b.c.c. phases of plutonium, because these phases have smaller numbers of atoms in the unit cells with less directional f-bonding character [3] and are best described by the LVP or EAM potential. Because the data for plutonium are very limited, we have used some structural data of δ-Pu and ϵ-Pu (Table 3) and some estimates of elastic constants (Table 4) as our basis for fitting our plutonium potential. This *preliminary* LVP is better at describing cubic phases of plutonium (*i.e.* δ-Pu and ϵ-Pu) than other phases of plutonium (*i.e.* α-Pu, β-Pu, γ-Pu

TABLE 3

Structural properties of plutonium [20, 24]. The melting temperature of plutonium is 640 °C and the boiling temperature is 3230 °C [20]

Element	Temperature (°C)	Pressure	Pearson symbol	Space group	Strukurbericht designation	Prototype	Lattice parameters (Å)			c/a or β
							a	b	c	
α-Pu	25	Atm.	$mP16$	$P2_1/m$	–	α-Pu	6.183	4.822	10.963	$\beta = 101.97°$
β-Pu	> 125	Atm.	$mI34$	$I2/m$	–	β-Pu	9.284	10.463	7.859	$\beta = 92.13°$
γ-Pu	> 215	Atm.	$oF8$	$Fddd$	–	γ-Pu	3.1587	10.162	10.162	–
δ-Pu (σ-Pu)	> 320	Atm.	$cF4$	$Fm3m$	A1 (f.c.c.)	Cu	4.6371	–	–	–
δ'-Pu (σ'-Pu)	> 463	Atm.	$tI2$	$I4/mmm$	A6 (b.c.t.)	In	3.3261	–	4.4630	$c/a = 1.3418$
ϵ-Pu	> 483	Atm.	$cI2$	$Im3m$	A2 (b.c.c.)	W	3.6343	–	–	–

TABLE 4

Experimental and estimated data of plutonium and fitted results of local volume potentials. Data in italics are estimations by comparison with nickel. The r.m.s. deviation of the fit is 1.3%

Property	Exp.	Fit or calc.	Deviation
δ-Pu phase (f.c.c.)			
a_0 (Å)	4.637	4.637	Exact
E_c (eV)	4.00	4.00	Exact
B (10^{12} dyn cm^{-2})	*0.6630*	0.6630	Exact
C_{11}	*0.9050*	0.9173	+1.36%
C_{12}	*0.5400*	0.5359	−0.76%
C_{44}	*0.4590*	0.4594	+0.09%
E_{vac} (eV)	*1.44*	1.45	+0.78%
ϵ-Pu phase (b.c.c.)			
a_0 (Å)	3.634	3.689	+1.51%
E_c (eV)	–	3.926	–
B (10^{12} dyn cm^{-2})	–	0.4900	–
C_{11}	–	0.3738	–
C_{12}	–	0.5482	–
C_{44}	–	0.4586	–
E_{vac} (eV)	–	1.39	–
D_0 (eV) of diatomic	*1.75*	1.803	+3.04%
R_0 (Å) of diatomic	*2.90*	2.918	+0.60%

Local volume potential parameters for Pu are: $D_M = 1.851371$ eV, $R_M = 2.79864$ Å, $\alpha_M = 1.33108$ Å^{-1}, $\beta = 2.8448$ Å^{-1}, $r_{cut} = 6.45585$ Å.

and δ'-Pu). Other phases of plutonium are less accurately described by LVPs (or the EAM potential), because the role of the angular dependence of the interactions may be more significant. We have listed some known properties in various phases of plutonium in Table 3 and 4. We used the experimental lattice constants (a_0) of δ-Pu and ϵ-Pu [20, 24] and the cohesive energy (E_c) of α-Pu [21], assuming that E_c of δ-Pu is not very different from that of α-Pu. The elastic constants (C_{11}, C_{12}, C_{44} and B) and vacancy energies are not available, so we use f.c.c. nickel as a reference material to derive the values for δ-Pu. We scale the elastic constants and bulk modulus with the surface energy based on the experimental linear correlation between surface energy and elastic constants [25]:

$$\frac{C_{ij}(\mathrm{Pu})}{C_{ij}(\mathrm{Ni})} = \frac{\Gamma_s(\mathrm{Pu})}{\Gamma_s(\mathrm{Ni})} \tag{8}$$

where the C_{ij} are the elastic constants in Voigt's notation and Γ_s is the surface energy of the (111) surface of the f.c.c. phase. The (111) surface was chosen as a reference surface to calculate the surface energy, because usually the (111) surface of f.c.c. metals has the lowest surface energy. The bulk modulus B scales in the same fashion as the other elastic constants.

The surface energy of nickel (2450 mJ m^{-2}) is taken from ref. 23. The energy of vacancy formation, E_{vac}, is scaled with the cohesive energy E_c:

$$\frac{E_{vac}(Pu)}{E_{vac}(Ni)} = \frac{E_c(Pu)}{E_c(Ni)} \tag{9}$$

The values of E_c were taken from ref. 21. Similarly, the diatomic distance R_0 and the cohesive energy D_0 scale with the lattice constant and cohesion of f.c.c. plutonium respectively:

$$\frac{R_0(Pu)}{R_0(Ni)} = \frac{a_0(Pu)}{a_0(Ni)} \tag{10}$$

$$\frac{D_0(Pu)}{D_0(Ni)} = \frac{E_c(Pu)}{E_c(Ni)} \tag{11}$$

Because the elastic constants and vacancy energies of δ-Pu are not known experimentally or theoretically, we used a self-looping fitting procedure in deriving the parameters for the LVPs for δ-Pu. We start fitting potentials by first assuming the (111) surface energy of δ-Pu is 1450 mJ m^{-2}; we first derive the initial estimated values for C_{ij} and B according to eqn. (8), then fit the potentials to these data. After we had generated the LVP potential, we used the potential to calculate the surface energy of the (111) surface of δ-Pu again. If the surface energy is different from the original assumed values, we then adjust the assumed value for surface energy and go through the fitting loop procedures again. We found that a final value for the (111) surface of δ-Pu of 895 mJ m^{-2} gives us "*self-consistency*" in surface energy and elastic constants. The "best" fit and the optimized parameters are shown in Table 4 and Fig. 2. Tables 3 and 4 show the experimental data used in the fits for δ-Pu and ϵ-Pu, along with the calculated values and the r.m.s. deviations of the fit (1.3%).

We have also listed some calculated elastic constants and cohesive and vacancy energies of the b.c.c. phase of ϵ-Pu. The elastic constants (C_{ij} and B as shown in Table 4) of ϵ-Pu are smaller than those of δ-Pu by about 25%. The vacancy energy of ϵ-Pu is 1.39 eV, which is slightly smaller than the vacancy energy of δ-Pu (1.45 eV). These results should be checked with new total energy band structure calculations or experimental measurements

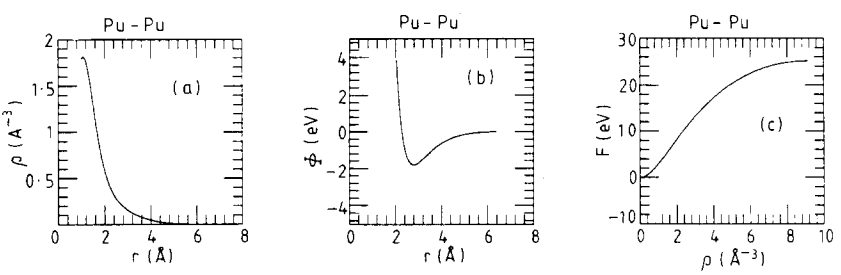

Fig. 2. Local volume potentials for plutonium: (a) $\rho(r)$, (b) $\phi(r)$ and (c) $F[\rho]$.

TABLE 5

Calculated relaxed surface energies Γ_s, for δ-Pu (f.c.c.) and α-Th (f.c.c.)[a]. $\Gamma_s(1\times2)$ is the surface energy of the 1×2 missing row surface obtained by removing every other row of $<1\,\bar{1}\,0>$ or $<1\,\bar{2}\,0>$ atoms. Thorium does not reconstruct on (110) or (210) surfaces, while δ-Pu may reconstruct on (210) but not on (110) surfaces. See refs. 13 and 14 for detailed discussion on surface reconstructions

	δ-Pu Γ_s (mJ m^{-2})	δ-Pu $\Gamma_s(1\times2)$ (mJ m^{-2})	α-Th Γ_s (mJ m^{-2})	α-Th $\Gamma_s(1\times2)$ (mJ m^{-2})
(111)	895	–	1860	–
(100)	943	–	1897	–
(110)	1047	1078	1982	2093
(210)	1099	1091	2013	2053

[a]Estimated values for surface energy are less than 2000 mJ m^{-2} for Pu and 1550 mJ m^{-2} for Th [23].

to test the accuracy of the potential. We also calculate the surface energies of many low index surfaces of δ-Pu (Table 5). We found that the (111) surface has the lowest surface energy of 895 mJ m^{-2} as expected and the (210) surface has the highest surface energy of 1099 mJ m^{-2}. These surface energies should be compared with an estimate of less than 2000 mJ m^{-2} for the plutonium surface using Miedema's method [23]. The large uncertainty in the estimated surface energy using Miedema's scheme is due to the lack of reliable information about the material. No definite conclusion on the quality of the potentials can be drawn at this point. We found (Table 5) that the (110) surface of δ-Pu does not favor the 1×2 missing row reconstructions like other f.c.c. metals such as gold, platinum and iridium (see refs. 13, 14 and references cited therein). We also found that the (210) surface of δ-Pu may favor the 1×2 missing row reconstruction as predicted for eight other f.c.c. metals (aluminum, nickel, copper, silver, palladium, platinum, gold and iridium) [13, 14]. These calculations for the surface energies and structures have to be taken only qualitatively because of the assumption that the elastic constants of δ-Pu scaled with those of f.c.c. nickel. We will test the LVP further on the structural and transport properties of δ-Pu and ϵ-Pu and the limits of the potential in describing other phases of plutonium (*i.e.* α-Pu, β-Pu, γ-Pu and δ'-Pu).

4. Discussion

Preliminary local volume potentials for the actinide metals thorium and plutonium have been generated by fitting experimental data and some theoretical estimates. These potentials fit available "experimental" data reasonably well. The r.m.s. deviations of the fit are rather small (in the range of 1%). Quantities such as elastic constants, cohesive energies and vacancy energies of the b.c.c. phases of thorium and plutonium have been calculated.

These calculations have to be checked by experiments or total energy calculations to determine the reliability of the potentials. The fit to plutonium is particularly difficult, because elastic constants and cohesive energies are not available. A self-looping procedure was used to derive a "self-consistent" fit to the elastic constants and surface energies. More reliable data on elastic constants, vacancy energies and cohesive energies of thorium and plutonium are needed. The present set of potentials (especially the potentials of plutonium) can be used with caution to give a rough idea of how the cubic phases of thorium and plutonium will behave. The potentials for thorium are better than those for plutonium. Tests of these potentials for other phases of plutonium by calculating the relative stability of α-Pu, β-Pu, γ-Pu, δ-Pu, δ'-Pu and ϵ-Pu as well as vacancy migration energies, surface energies, surface reconstructions and phase changes under various combinations of pressure and temperature, together with tests on thorium, will be presented in a future publication. As new and reliable data or calculations on elastic constants and cohesive energies for plutonium and thorium become available, a new set of potentials will be fitted. If we find that local volume potentials are not capable of describing plutonium and thorium, we will examine the applicability of tight-binding approaches in the empirical forms of Tersoff [26] and Pettifor [27] or the *ab initio* form of Andersen and Jepsen [28].

Acknowledgments

I would like to thank A. M. Boring, O. Eriksson, J. M. Wills, R. C. Albers, G. Straub and J. L. Smith for helpful discussions and R. Lesar for bringing this subject to my attention. This work is performed under the auspices of the US Department of Energy.

References

1 A. J. Freeman and C. Keller (eds.), *Handbook on the Physics and Chemistry of the Actinides*, Vol. 3, North-Holland, Amsterdam, 1985.
2 A. J. Freeman and G. H. Lander (eds.), *Handbook on the Physics and Chemistry of the Actinides*, Vol. 1 and 2, North-Holland, Amsterdam, 1985.
3 J. L. Smith, Z. Fisk and S. S. Hecker, *Physica B, 130* (1985) 151.
4 L. Manes (eds.), *Actinides—Chemistry and Physical Properties, Structure and Bonding 59/60*, Springer, Berlin, 1985.
5 N. M. Edelstein (ed.), *Actinides in Perspective*, Pergamon, Oxford, 1982.
6 A. J. Freeman and J. B. Darby Jr. (eds.), *The Actinides: Electronic Structure and Related Properties*, Vols. 1 and 2, Academic, New York, 1974.
7 J. M. Wills and O. Eriksson, *Phys. Rev. B.*, in the press.
8 A. F. Voter and S. P. Chen, *MRS Symp. Proc., 82* (1987) 175.
9 M. S. Daw and M. I. Baskes, *Phys. Rev. B, 29* (1984) 6443.
10 S. P. Chen, D. J. Srolovitz and A. F. Voter, *J. Mater. Res., 4* (1989) 62.
11 S. P. Chen, A. F. Voter, R. C. Albers, A. M. Boring and P. J. Hay, *J. Mater. Res., 5* (1990) 955.

12 J. K. Norskov and N. D. Lang, *Phys. Rev. B, 21* (1980) 2131.
M. J. Stott and E. Zaremba, *Phys. Rev. B, 22* (1980) 1564.
13 S. P. Chen and A. F. Voter, *Surf. Sci. Lett., 244* (1991) L107.
S. P. Chen, *Mater. Sci. Eng. B, 6* (1990) 113.
14 S. P. Chen, *Philos. Mag. A*, in the press.
15 R. J. Harrison, A. F. Voter and S. P. Chen, in V. Vitek and D. J. Srolovitz (eds.), *Atomistic Modeling of Materials: Beyond Pair Potentials*, Plenum, New York, 1989, pp. 219–222 (for iron).
R. J. Harrison, F. Spaepen, A. F. Voter and S. P. Chen, Innovations in ultrahigh-strength steel technology, in G. B. Olsen, M. Azvin and E. S. Wright (eds.), *Proc. 34th Sagamore Army Materials Research Conf., Lake George, NY, August–September 1987*, US Army Materials Technology Laboratory, Watertown, MA, 1990, pp. 651–675 (for iron).
S. P. Chen, to be published (for iron, niobium, chromium, tungsten and molybdenum).
16 S. P. Chen, *Surf. Sci. Lett, 264* (1992) L162.
17 S. M. Foiles, *Phys. Rev. B, 32* (1985) 7685.
18 S. M. Foiles, M. I. Baskes and M. S. Daw, *Phys. Rev. B, 33* (1986) 7983.
19 J. H. Rose, J. R. Smith, F. Guinea and J. Ferrante, *Phys. Rev. B, 29* (1984) 2963.
20 T. B. Massalski (eds.), *Binary Alloy Phase Diagrams*, American Society for Metals, Metals Park, OH, 1986, pp. 2176, 2181.
21 C. Kittel, *Introduction to Solid State Physics*, Wiley, New York, 5th edn., 1976.
22 R. O. Simmons and H. Wang, *Single Crystal Elastic Constants and Calculated Aggregate Properties: A Handbook*, MIT Press, Cambridge, MA, 1971.
23 F. R. deBoer, R. Boom, W. C. M. Mattens, A. R. Miedema and A. K. Niessen, *Cohesion in Metals: Transition Metal Alloys*, North-Holland, Amsterdam, 1989.
24 R. B. Roof, *Los Alamos National Laboratory Rep. LA-7006-MS*, 1977.
25 L. E. Murr, *Interfacial Phenomena in Metals and Alloys*, Addison-Wesley, Reading, MA, 1975.
26 J. Tersoff, *Phys. Rev. B, 39* (1989) 5566.
27 D. G. Pettifor, *Phys. Rev. Lett., 63* (1989) 2480.
28 O. K. Andersen and O. Jepsen, *Phys. Rev. Lett., 53* (1984) 2571.